Classification of stages of wear in spur gears based on wear debris morphology

Dharmender[1], Ashish K. Darpe[2], and Harish Hirani[3]

[1,2]*Department of Mechanical Engineering, Indian Institute of Technology, Delhi, New Delhi, 110016, India*
dkj6217@gmail.com
akdarpe@mech.iitd.ac.in

[3]*Central Mechanical Engineering Research Institute – CSIR, Durgapur, West Bengal, 497118, India*
hirani@mech.iitd.ac.in

ABSTRACT

This work investigates the morphological changes in the wear debris, generated during the different stages of gear wear. Wear debris are generated at the mating load-bearing tooth surfaces having relative motion. The number and size of collected wear debris provide useful information for the gear fault diagnosis.

In the present work, both online and offline analyses of wear debris are carried out for gear fault diagnosis. In the online analysis, the oil from the gear sump is passed through online wear debris counter (to estimate the number of wear particles per minute) and particle size bin. Along with the online process, the oil samples are collected periodically, and wear debris particle images are captured using a scanning electron microscope (SEM). These images are subsequently processed to determine the parameters related to the shape, size and boundary features of the particles. The results of the modified texture in different stages of gear wear are reported. The average wear mass calculated as the actual area of the wear particles is combined with particle per minute is used as the stage's classification.

The combined online and offline study provides a better prediction of mild wear progression along with the information on the wear mechanisms at different stages of wear. The presence of different type of particles (ferrous and non-ferrous) points to degradation of specific components.

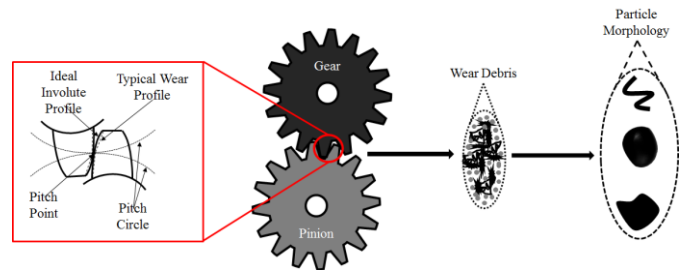**KEYWORDS:** Spur gear, wear debris, particle morphology, fractal analysis

Figure 1. Schematic diagram showing wear debris generation interface and particle morphology

1. INTRODUCTION

Geared transmission system is widely used in many applications including aviation, wind turbine, industrial, civilian and military application (Liang, Zuo, & Feng, 2018). Over a period of time wear debris is generated at the relative moving surfaces of load sharing gear teeth (Davies, 1998) and hence the gear tooth surface degrades with time. The generated wear debris carry valuable information regarding the wear mechanism, damage progression and location in the gearboxes. The wear debris is classified based on quantity, quality, morphology, the color and material properties of wear debris (Khan & Starr, 2006; M. Kumar, Shankar Mukherjee, & Mohan Misra, 2013; Myshkin, Kwon, Grigoriev, Ahn, & Kong, 1997).

Traditionally, the wear debris analysis is carried out offline after periodic gearbox oil sample collection. However, nowadays, a metallic wear debris sensor is used in an online mode to evaluate the progression of debris in the gearbox. The concentration of the metallic particles in oil correlates well with the severity of the fault (Dempsey & J., 2003; Dempsey, Lewicki, & Le, 2007; Kattelus, Miettinen, & Lehtovaara, 2018; P. Kumar, Hirani, & Agrawal, 2018; Yan, Youbai, Fang, & Zhigang, 1998). In the offline analysis of the sample, the ferrographic plates are prepared to perform scanning electron microscope (SEM) imaging, and different

wear particles are characterized under the SEM to assess the mode of formation (Muniyappa, Chandramohan, & Seethapathy, 2010; Scott, 2003). In some studies, visual inspection of the particles was carried out to detect the wear mechanism (Ebersbach, Peng, & Kessissoglou, 2006).

The geometrical parameters of a wear particle such as area, perimeter, fiber ratio, etc. are used to characterize the wear particles. The surface texture based pattern is used to classify these particles (Laghari, 2003; Zhongxiao Peng, 2002; Stachowiak, Stachowiak, & Podsiadlo, 2008). Different fractal techniques are used to find the boundary texture of the wear debris (M. Kumar et al., 2013; Podsiadlo & Stachowiak, 2000). (Iwai et al., 2010) studied the distribution of size and number of the wear particles in oil as a function of sliding distance.

The particle is assumed as spherical to calculate the wear mass in the previous on-line particle progression studies (Dempsey, Lewicki, & Decker, 2004). Many researchers only considered the number of wear debris particles (Kattelus et al., 2018). The type of wear particle is essential to track the source of particle generation.

This article investigates the change in the morphological parameters of the wear debris generated during different stages of the gear tooth surface wear. The ferrous and non-ferrous particles in metallic wear debris sensor have a different source of generation. The SEM images of the debris are processed to determine parameters such as area, perimeter, circularity, aspect ratio, roundness, mean value, standard deviation, skewness, kurtosis, boundary fractal using image analysis software. The average wear mass in each stage is calculated using an average area of the wear particles from the calculated parameters of the particle morphology. The evolution of these parameters with time and its correlation with different stages of the gear tooth surface wear is studied in this study. The combination of online and offline results can be very useful for gear condition monitoring.

2. EXPERIMENTAL SETUP

An experimental test rig, shown in Figure 2, is used to perform the experiments. The gearbox has a step-down ratio of 1.96 and is driven by a 30 kW DC motor. The motor is controlled by 3-phase 440 V / 75 A motor controller. The output of the gearbox is attached to water-cooled eddy current dynamometer (E-50) of torque capacity 200 Nm. The specification of the gears used for the test is given in Table 1.

The test was conducted at a speed of 1200±50 RPM, load 40±2 Nm, stable oil sump temperature of 40±2℃, the surrounding temperature of 18±2℃ for 208 hours. Although the speed was maintained around the rated speed, there was some inherent speed fluctuation is due to controller output to the driver, the ripple in DC motor, error in the drive (gear drive), and the variation in the load at the output shaft. During the test, the continuous wear data (wear particle per minute and particle size distribution) of the gearbox were acquired. The gearbox operation was paused to collect oil samples from gearbox after every 40 hours. The interval of offline sampling is decided based on experiments performed and block on disc instrument with a sample of same properties start showing the stable friction value around 40 hours. The oil samples were collected at a stable operating temperature. For the replenishment of the bled oil sample, every time a 10 ml of fresh oil of the same properties is first brought to the temperature of the sump externally and then refilled to the sump. Since the gearbox sump capacity is 2000 ml, the 10 ml oil sample extracted for offline study is only 0.005% of the total sump oil amount. It is thus expected that this minuscule amount of the oil replacement would not bring any significant change in the oil properties, such as viscosity, etc and would not also alter the wear particle data. The samples were processed within 48 hours of the collection, and the wear debris were harvested from the lubricant sample using established methodology and then used for the SEM analysis. The experiment is terminated when the number of wear particles starts fluctuating more and increasing trend.

For acquiring online wear debris data, a Kittiwake make metallic wear debris sensor (AS-19144-KW) was used.

Parameter	Pinion	Gear
Number of teeth	27	53
Pitch diameter (mm)	54	106
Base diameter (mm)	50.7	99.6
Center distance (mm)	80	
Module (mm)	2	
Face width (mm)	20	
Pressure angle (°)	20	
Contact ratio	1.6	
Material properties		
Material	EN 24	
Rockwell hardness number without hardening (HRC)	20	
Rockwell hardness number hardening (HRC)	58	
Poisson's ratio	0.3	
Young modulus (GPa)	207	
Kinematic viscosity (@ 100°C, cSt)	13.5-18.5	

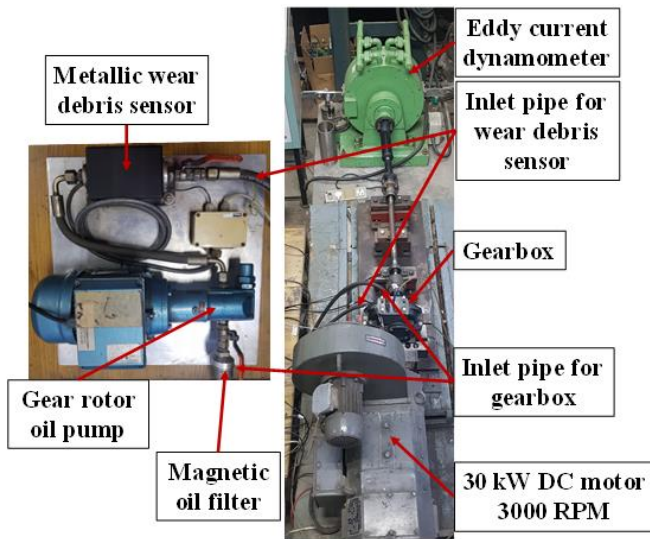Table 1. Test gear dimension and specification

Figure 2. Experimental setup

3. RESULT AND DISCUSSION

3.1. ONLINE STUDY

The online particle monitoring is implemented using the wear debris sensor system connected to the gearbox oil-outlet. The oil debris sensor records a count of wear particles in bins with a range of particle size. The range of the bin sizes in microns is shown in Table 2. The wear debris data of 208 hours from the start of the experiment is collected. At the initial stage of run-in (0-40 hours), the wear rate is expectedly high with fluctuation in the range of 0-150 ppm (particles per minute) as noted from Figure 3. The wear rate shows a decline (in stage 2) to a more or less stagnant level of 40 ppm with a slight spike during 70-80 hrs. It has been found that during the initial phase (till 40 hours of operation) the <50µm size ferrous and large size non-ferrous of size >250µm particles are found to be the dominating contributors to the wear debris. This stage is the run-in stage and is mainly responsible for the smoothening of the tooth surface. In stage 3 the number of wear particles quickly jumps to a new level of 75 ppm with some fluctuation. After 160 hours of operation, the wear particles show a sharp and sudden increase and thereafter shows an overall increasing trend with significant intermittent fluctuation. In both stages 3 and 4, the ferrous particle with <100µm size and non-ferrous particles with <250µm size were the dominating contributor.

The total span shows distinct differences in the trend of wear rates. After a fluctuation in wear particles in the initial stage, it shows continuous decline towards the end of the first stage, in stages 2 and 3, the wear rate (in ppm) is nearly stagnant slope, but with a higher rate in stage 3. The wear rate stage 4

shows an upward trend, most probably due to continuous surface damage of the gear tooth.

The ferrous particles were measured and classified under three different size classes (0-50µm, 50-100µm and 100-400µm) as mentioned in Table 2. Similarly, the non-ferrous particles were measured and classified (0-150µm, 150-250µm and 250-400µm). The mean of the range of size of wear particles in the bin number represents the average particle size of the bin, as shown in the table. An hourly record of the number of particles measured by the sensor is used to find the average number of ferrous and non-ferrous wear particles in an hour in each stage and are shown in Figures 4 and 5. For example, for stage I, there are 40 readings (one reading for each hour of operation) for the 40-hour stage-I phase of the wear. The average number of particles for stage-I is the arithmetic mean of such 40 particle count readings. The corresponding standard deviation is also obtained for each phase. The error bar shown for each particle size in each stage represents the standard deviation. The distribution of the wear debris particles in these figures indicates the dominant particle size in each of the stages. It is clear from Figure 4 that the smaller particle size (average size 25 micron) mainly dominates the wear debris in initial run-in condition (stage 1) with more than average 7000 particles per hour, while they are less than the average 1800 particles per hour in other stages. It is clear that as the wear progresses after the initial run-in period, the wear particles of 75-micron size start increasing monotonically, and they are found to be the true indicator of wear progression. In comparison, the smaller size particles, as well as bigger particles, do not show a significant and consistent increase. For the nonferrous particles, the trend is similar for medium size (75 micron) particles, with smaller size particles also showing a monotonic trend.

The type of particle indicates the source of the particle generation. The ferrous particles are mainly from the gear tooth surface while the non-ferrous particles could be from the shaft seals. The seal is in continuous rub against the gear shaft.

Bin Number	Ferrous Particle		Non-Ferrous Particle	
	Bin Range (µm)	Average particle size (µm)	Bin Range (µm)	Average particle size (µm)
1	0-50	25	0-150	75
2	50-100	75	150-250	200
3	100-400	250	250-400	325

Table 2. Wear debris particle size ranges

In Figure 6, the average wear particles and the average wear mass are plotted. Average wear mass is a function of the average area (From Table 3), the average number of particles per hour, average particle size, and density of the gear material used. A density value of 7840 kg/m^3 is used to calculate the average wear mass in each stage. The wear mass for the stages 1 to 4 are 0.2885 mg/hour, 0.0408 mg/hour, 0.3923 mg/hour and 0.8679 mg/hour, respectively. The particles in stage 1 and stage 4 are nearly similar in the count, but the difference in wear mass is nearly 4 times, which could be due to the fact that smaller size (25µm) particles dominate stage 1, while in stage 4 the particles of larger size (75µm) dominate.
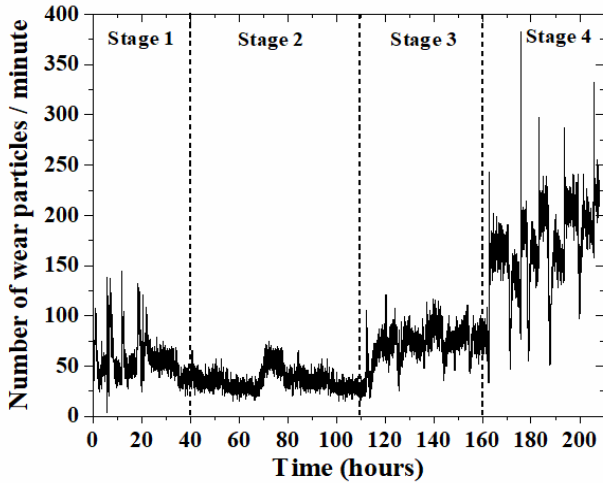

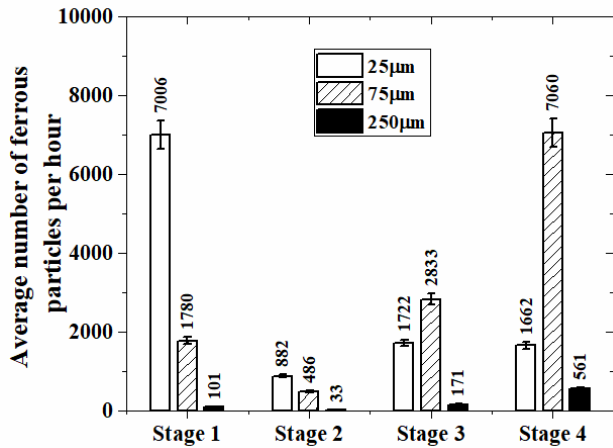Figure 3. Wear particle per minute obtained during the 0-208 hours of operation

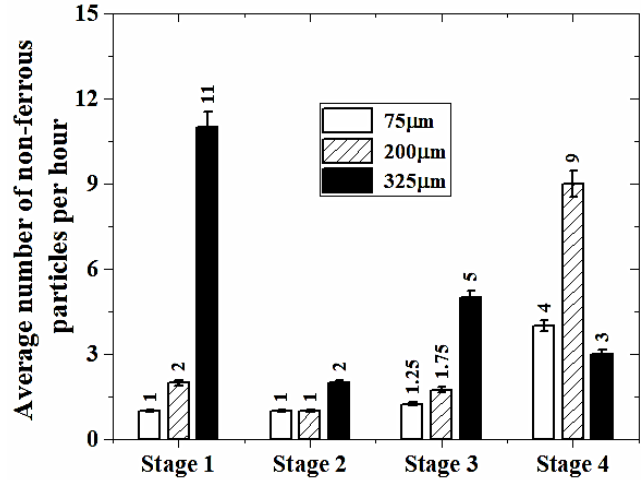Figure 4. Ferrous wear particles distribution
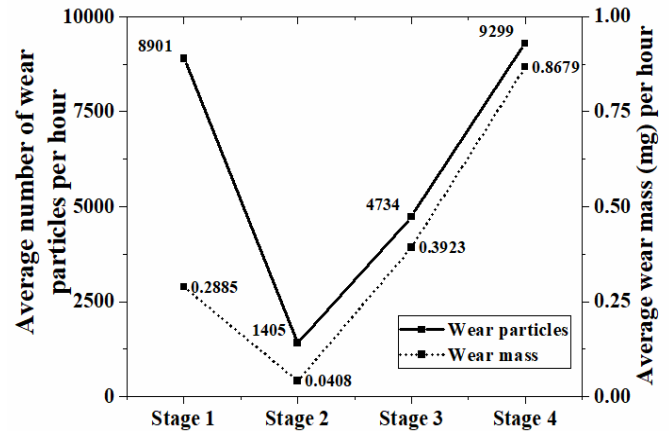

Figure 5. Non-ferrous wear particles distribution

Figure 6. Trend of average wear particles and wear mass across different stages

3.2. OFFLINE STUDY

In the offline study, the oil samples were collected periodically; after every 40 hours of operation. The wear debris, harvested from the oil sample, were analyzed under the Scanning Electron Microscope (SEM). The SEM images were processed in an image processing tool (ImageJ) to extract the morphological parameters (Figure 7). The raster cell size chosen is 5 µm^2 for stages 1 and 2, while due to the increased wear particle sizes in stages 3 and 4, it was increased to 20 µm^2. Through a separate study conducted, it is found that the change in the raster cell size does not significantly influence the values of the parameters computed. The images were processed to extract various morphological feature parameters of the wear debris particles. These parameters are as follows:

Aspect ratio: it is a measure of the elongation of a boundary profile and is quantified by the ratio of length and breadth of the particle(Z. Peng & Kirk, 1998).
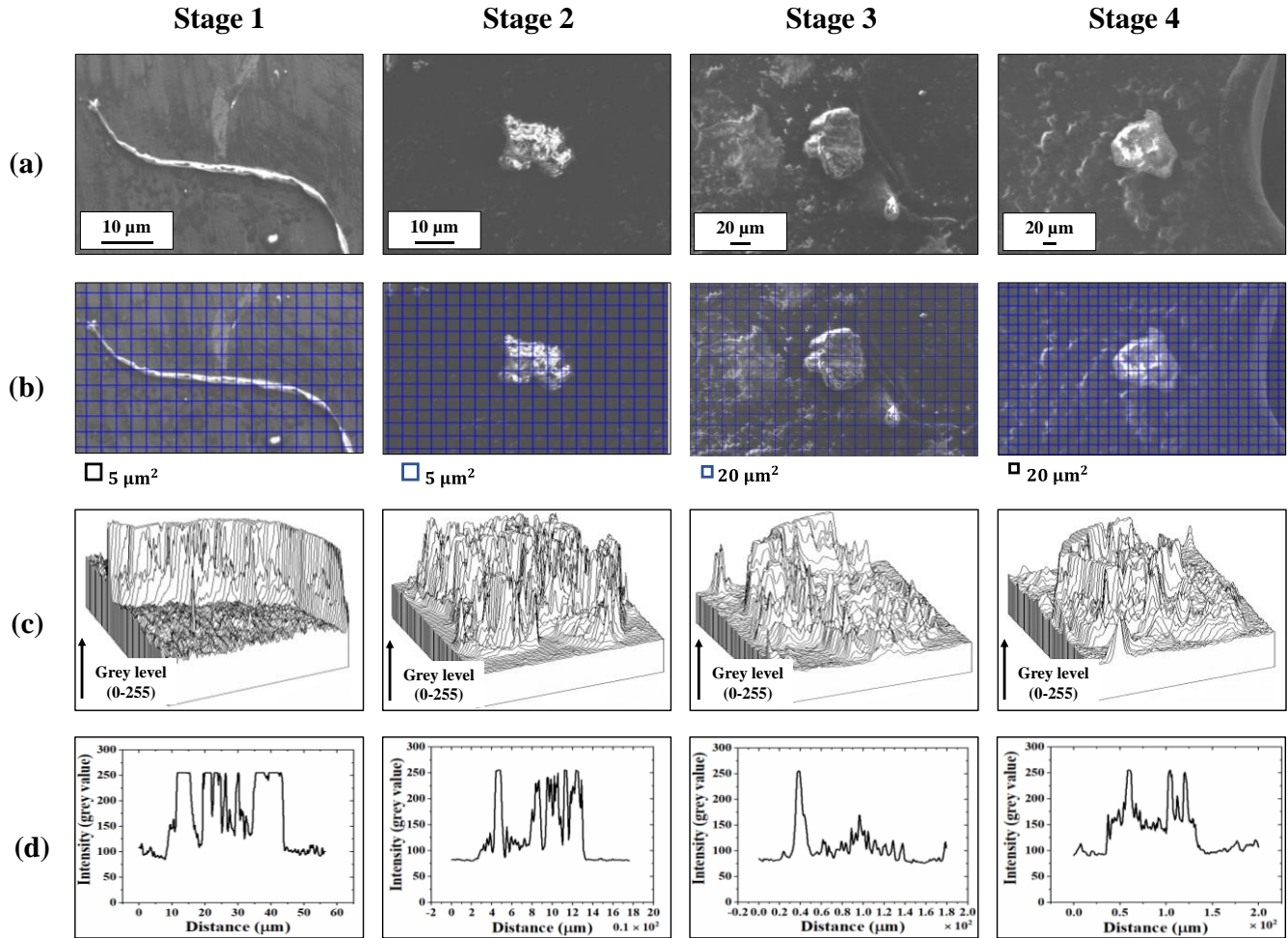
Figure 7. Different type of particle obtained for duration 0-208 hours (a) SEM image of particles (b) shape parameter evaluation by fractal analysis (c) surface plot and (d) profile plot

Roundness: the roundness is given by (4(projected area)/ π (length)^2) and is sensitive to elongation (Z. Peng & Kirk, 1998). It is obvious that as the particle deviates from the round shape the roundness reduces from an ideal value of 1 (for circle) to a theoretical lowest value of 0.

Solidity (area/convex area) imply the ruggedness of a boundary profile. The solidity is 1 for the particle that has no concavities and it is less for particles with indentations (Kirk, Panzera, Anamalay, & Xu, 1995).

Standard deviation (SD $= \sqrt{\sum_{i=1}^{n} \delta_i^2/(n-1)}$)is the deviation (δ) of the minimum circle fit when moving along the coastline of the particle. The other moment parameters are skewness ($\sum_{i=1}^{n} \delta_i^3/nSD^3$), Kurtosis ($\sum_{i=1}^{n} \delta_i^4/nSD^4$) (Yuan, Chin, Hua, Dong, & Wang, 2016).

Boundary fractal is a numerical parameter used for characterizing of the boundary of wear particle by enclosing the wear particle by a polygon of constant sides (Podsiadlo & Stachowiak, 1998).

To analyze particle morphology, the SEM images, and the surface plot and the profile plot for particles in each stage were obtained and are shown in Figure 7. The surface plots are obtained using the three-dimensional fast Fourier transform (FFT). To obtain the FFT 3D plots, as shown in Figure 7 (c), the surface is segmented in small data points, and points were transformed using FFT, row by row and stacked together to obtain 3 D transformed plot. The vertical line shows the grey level intensity of the pixel at that point. The profile plot is 1D FFT plot along the line connecting two points on the wear particle contour. The height (y-axis) shows

Property	S1P (mean)	S1P (standard deviation)	S2P (mean)	S2P (standard deviation)	S3P (mean)	S3P (standard deviation)	S4P (mean)	S4P (standard deviation)
Area (μm^2)	99.4	2.15	69.5	1.89	158.83	3.38	153	2.93
Perimeter (μm)	86.86	3.76	97.3	0.92	189.27	3.89	171.36	1.29
Major axis (μm)	27.4	1.48	11.3	0.16	15.3	1.02	14.8	2.02
Minor axis (μm)	4.63	0.67	7.82	0.09	12.74	1.20	13.2	0.44
Circularity	0.05	0.007	0.61	0.03	0.778	0.03	0.75	0.05
Aspect ratio	5.91	0.23	1.4	0.02	1.199	0.02	1.12	0.013
Roundness	0.16	0.004	0.69	0.004	0.827	0.016	0.89	0.017
Solidity	0.17	0.016	0.80	0.02	0.9354	0.019	0.90	0.05
Mean	188	2.41	160	1.64	127.87	1.50	163	1.92
Standard deviation	56.5	2.06	34.4	0.42	39.02	1.13	41	2.47
Skewness	9.03	0.77	4.8	0.30	1.754	0.02	1.04	0.02
Kurtosis	14.9	0.21	6.25	0.05	5.204	0.167	9.96	0.65
Boundary fractal	6.8	0.33	1.24	0.02	1.462	0.196	1.6	0.25

Table 3. The mean and standard deviation values of the particle morphological parameters for particles in each stage of gear life

the grey level spectral intensity. The surface plot of the stage 1 particle is shown more laminar morphology on the surface and more irregularities on the contour. The spectral intensities of the laminar wear particles are evenly distributed. The profile plot in Figure 7 (d) corresponds to the surface plot in Figure 7 (c) of stage 1 displays the same evenly distributed spectral densities with the nearly same height. The particles in stages 2 and 3 exhibits a surface that has rugged topography, and the surface is no longer laminar. The spectral densities distribution is no longer evenly distributed but aligned in one direction for surface plot and profile plot. In stage 4, the surface is very rough but less chaotic at boundaries. The spectral density distribution is non-uniform distribution and non-even directional alignment for both surface and profile plots. The particle obtained in stage 4 exhibits an abrasive particle characteristic.

The surface plot for different orientation of the wear particles are given in APPENDIX -I. The surface plot, profile plot, along with the statistical parameters, shows that the existence of different wear mechanism. At stage 1 – cutting was dominating and resulted in a smooth surface (Figure 7). The spiral cutting particles (as shown in Figure 7 (a)) are obtained in stage 1 confirm the dominance of cutting wear mechanism.

The wear particles generated at stage 1, were trapped at the interface, resulting in the three-body abrasion at stage 2 and 3. The particle images in stages 2 and 3 show the modification in the wear debris morphology.

In Table 3, the different particle morphological parameters are listed. The S1P (Stage 1- particle), S2P (Stage 2- particle), S3P (Stage 3- particle), and S4P (Stage 4- particle) are the particles obtained during the different stages corresponding to stage 1, stage 2, stage 3, and stage 4 respectively. From the Table 3, it can be observed that particle obtained in stage 1 are cutting particle and are of fiber structure with low circularity, roundness, solidity and high values of aspect ratio, mean, standard deviation, skewness, kurtosis and fractal dimension which shows the chaotic boundary. The particles get modified with the time and show that in stage 4 particles become more in circular shape with low values of aspect ratio, mean, standard deviation, skewness, kurtosis and fractal dimension which shows the chaotic boundary.

It is noticeable from the above study that a particle size of less than 100µm (Davies, 1998; Kattelus et al., 2018) is dominating contributor to the wear debris and indicates the existence of mild wear. It is noticeable that the particles

morphological modification in parallel with on-line monitoring is a promising way to follow the progression of mild wear. The on-line particle progression provides the information regarding the stage changes in the damage of the gear along with average wear mass (Figure 6). The offline study of the particle morphological modification gives information about the change in the surface profile of the wear particle and existing wear mechanism.

4. CONCLUSION

The online and offline studies of the wear debris provide a better prediction of the progression and the change in wear mechanisms at a different stage. The presence of the non-ferrous particle in the system indicates degradation of other components along with the gear. The result shows that the concentration of wear debris particles in oil is well correlated to the wear mass.

- The accumulation and the time of occurrence of the wear particles are traced out with the help of an online particle counter.

- The presence of non-ferrous particles may be due to seal wear (continuously rubbing against the gear rotor) or bearing degradation.

- The progressive damage of the gear tooth surface is confirmed by the increase in the number of wear particles and the average wear mass. The particle of an average size of 75 micron are found to be the right candidate to track the trend of wear of gear tooth surface.

- In the initial stage, the particles are in fiber shape due to cutting action. In stage 2 and 3, the particles are semi-laminar due to the three-body abrasion. In stage 4, the particles are no longer laminar as a result of two-body abrasion.

- SEM images of particles conclude that profile of the wear particles gets modified over time, and the surface gets rougher.

The initial work on a combination of online and offline wear debris classification presented in this work can aid and complement the other methods of gear condition monitoring. In future studies, these results can be further combined with other sensors (vibration, and acoustic) data better to predict the condition of the gearbox under mild wear progression.

REFERENCES

Davies, A. (1998). *Handbook of Condition Monitoring*. Springer-science+ Business Media, B.V.

Dempsey, & J., P. (2003). Integrating oil debris and vibration measurements for intelligent machine health monitoring. NASA/TM—2003-211307 (https://ntrs.nasa.gov/search.jsp?R=20030056593)

Dempsey, P. J., Lewicki, D. G., & Decker, H. J. (2004). Investigation of Gear and Bearing Fatigue Damage Using Debris Particle Distributions. *Nasa / Tm - 2004-212883 Arl-Tr-3133*, *298*(0704), 16.

Dempsey, P. J., Lewicki, D. G., & Le, D. D. (2007). Investigation of current methods to identify helicopter gear health. *IEEE Aerospace Conference Proceedings*, (July). https://doi.org/10.1109/AERO.2007.352844

Ebersbach, S., Peng, Z., & Kessissoglou, N. J. (2006). The investigation of the condition and faults of a spur gearbox using vibration and wear debris analysis techniques. *Wear*, *260*(1–2), 16–24. https://doi.org/10.1016/j.wear.2004.12.028

Innovation eliminates motor speed ripple | Machine Design. (n.d.). Retrieved June 19, 2020, from https://www.machinedesign.com/motors-drives/article/21828806/innovation-eliminates-motor-speed-ripple

Iwai, Y., Honda, T., Miyajima, T., Yoshinaga, S., Higashi, M., & Fuwa, Y. (2010). Quantitative estimation of wear amounts by real time measurement of wear debris in lubricating oil. *Tribology International*, *43*(1–2), 388–394. https://doi.org/10.1016/j.triboint.2009.06.019

Kattelus, J., Miettinen, J., & Lehtovaara, A. (2018). Detection of gear pitting failure progression with on-line particle monitoring. *Tribology International*, *118*(February), 458–464. https://doi.org/10.1016/j.triboint.2017.02.045

Khan, M. A., & Starr, A. G. (2006). Wear debris: Basic features and machine health diagnostics. *Insight: Non-Destructive Testing and Condition Monitoring*, *48*(8), 470–476. https://doi.org/10.1784/insi.2006.48.8.470

Kirk, T. B., Panzera, D., Anamalay, R. V., & Xu, Z. L. (1995). Computer image analysis of wear debris for machine condition monitoring and fault diagnosis. *Wear*, *181–183*(PART 2), 717–722. https://doi.org/10.1016/0043-1648(95)90188-4

Kumar, M., Shankar Mukherjee, P., & Mohan Misra, N. (2013). Advancement and current status of wear debris analysis for machine condition monitoring: a review. *Industrial Lubrication and Tribology*, *65*(1), 3–11. https://doi.org/10.1108/00368791311292756

Kumar, P., Hirani, H., & Agrawal, A. K. (2018). Online condition monitoring of misaligned meshing gears using wear debris and oil quality sensors. *Industrial Lubrication and Tribology*, *70*(4), 645–655. https://doi.org/10.1108/ILT-05-2016-0106

Laghari, M. S. (2003). Recognition of texture types of wear particles. *Neural Computing and Applications*, *12*(1), 18–25. https://doi.org/10.1007/s00521-003-0367-y

Liang, X., Zuo, M. J., & Feng, Z. (2018). Dynamic modeling of gearbox faults: A review. *Mechanical Systems and Signal Processing*, *98*, 852–876. https://doi.org/10.1016/j.ymssp.2017.05.024

Muniyappa, A., Chandramohan, S., & Seethapathy, S.

(2010). Detection and Diagnosis of Gear Tooth Wear through Metallurgical and Oil Analysis. *Tribology Online*, *5*(2), 102–110. https://doi.org/10.2474/trol.5.102

Myshkin, N. K., Kwon, O. K., Grigoriev, A. Y., Ahn, H. S., & Kong, H. (1997). Classification of wear debris using a neural network. *Wear*, *203–204*(96), 658–662. https://doi.org/10.1016/S0043-1648(96)07432-7

Peng, Z., & Kirk, T. B. (1998). Computer image analysis of wear particles in three-dimensions for machine condition monitoring. *Wear*, *223*(1–2), 157–166. https://doi.org/10.1016/S0043-1648(98)00280-4

Peng, Zhongxiao. (2002). An integrated intelligence system for wear debris analysis. *Wear*, *252*(9–10), 730–743. https://doi.org/10.1016/S0043-1648(02)00031-5

Podsiadlo, P., & Stachowiak, G. W. (1998). Evaluation of boundary fractal methods for the characterization of wear particles. *Wear*, *217*(1), 24–34. https://doi.org/10.1016/S0043-1648(98)00168-9

Podsiadlo, P., & Stachowiak, G. W. (2000). Scale-invariant analysis of wear particle surface morphology II. Fractal dimension. *Wear*, *242*(1–2), 180–188. https://doi.org/10.1016/S0043-1648(00)00417-8

Scott, D. (2003). Debris examination — a prognostic approach to failure prevention. *Wear*, *34*(1), 15–22. https://doi.org/10.1016/0043-1648(75)90304-x

Stachowiak, G. P., Stachowiak, G. W., & Podsiadlo, P. (2008). Automated classification of wear particles based on their surface texture and shape features. *Tribology International*, *41*(1), 34–43. https://doi.org/10.1016/j.triboint.2007.04.004

Yan, L., Youbai, X., Fang, Z., & Zhigang, Y. (1998). Revision to the concept of equilibrium concentration of particles in lubrication system of machines. *Wear*, *215*(1–2), 205–210. https://doi.org/10.1016/S0043-1648(97)00269-X

Yuan, W., Chin, K. S., Hua, M., Dong, G., & Wang, C. (2016). Shape classification of wear particles by image boundary analysis using machine learning algorithms. *Mechanical Systems and Signal Processing*, *72–73*, 346–358. https://doi.org/10.1016/j.ymssp.2015.10.013

BIOGRAPHIES

Dharmender is currently pursuing doctoral research at Indian Institute of Technology Delhi, India working in the Vibration Research Laboratory. He received his M. Tech Degree in Machine Design from National Institute of Technology. His current research focuses on the fault assessment of spur gears. His research interests are condition monitoring and tribological studies of machine elements.

Ashish K Darpe is Professor in the Department of Mechanical Engineering at Indian Institute of Technology Delhi, India. His research interest includes the condition monitoring, fault diagnosis, prognosis and rotor dynamics. He has published more than 70 research papers in the field of vibrations, fault diagnosis, rotor dynamics and condition monitoring.

Harish Hirani is Director of CSIR- Central Mechanical Engineering Research Institute, Durgapur, India. He is also Professor in the Department of Mechanical Engineering at Indian Institute of Technology Delhi, India. His research interest includes magnetic bearings, journal bearings, magnetorheological fluids, mechanical seals, condition monitoring, fault diagnosis and prognosis. He has published more than 80 research paper in the field of tribology and condition monitoring.

APPENDIX-I

The surface plot of the particles at a different orientation.